IEEE Access
Multidisciplinary ⋮ Rapid Review ⋮ Open Access Journal

Received 25 December 2024, accepted 10 February 2025, date of publication 17 February 2025, date of current version 21 February 2025.

Digital Object Identifier 10.1109/ACCESS.2025.3542451

RESEARCH ARTICLE

Transformative Transfer Learning for MRI Brain Tumor Precision: Innovative Insights

RAJA WASEEM ANWAR[1], MOHAMMAD ABRAR[2], (Senior Member, IEEE), AND FAIZAN ULLAH[3]

[1]Department of Computer Science, German University of Technology in Oman, Muscat 130, Oman
[2]Faculty of Computer Studies, Arab Open University, Muscat 122, Oman
[3]Forschungszentrum Jülich, Institute of Neuroscience and Medicine, 52428 Jülich, Germany

Corresponding author: Raja Waseem Anwar (raja.anwar@gutech.edu.om)

This work was supported by German University of Technology in Oman (GUtech), Muscat, Oman, under the Seed Grant SG/23/NR/CS/RA.

ABSTRACT Accurate brain tumor detection is essential for effective treatment and improved patient outcomes, yet conventional MRI classification methods often struggle with complex and variable imaging data. This study introduces the Transformative Transfer Learning (TTL) model, leveraging pre-trained deep neural networks fine-tuned for MRI brain tumor classification, using datasets from Nickparvar and Cheng. High-quality inputs were achieved through preprocessing, including resizing, normalization, noise reduction, and data augmentation. The TTL model, employing architectures such as VGG16, ResNet-50, InceptionV3, and DenseNet-121, demonstrated a substantial improvement over traditional methods, achieving an accuracy of 94.5%, sensitivity of 92.8%, and specificity of 93.1%. Additionally, the model yielded a precision of 93.2%, recall of 92.8%, F1-score of 93.0%, and true positive and true negative rates of 92.8% and 93.1%, respectively. Training and validation loss values of 0.15 and 0.18 confirm effective model convergence. These metrics underscore the model's potential as a robust tool in clinical diagnostics, providing a pathway to more accurate and efficient MRI-based brain tumor detection.

INDEX TERMS Brain tumor detection, transformative transfer learning, MRI, deep learning, transfer learning, medical imaging.

I. INTRODUCTION

The intricacy of the human brain, which is held responsible for an extensive array of functions, i.e., from emotion to cognition, stands out against its vulnerability to several diseases and circumstances. Particularly among all these, the brain tumor emerges as a striking disease because of its potential sternness and the complications are inherent in its detection and cure. Brain tumors signify the abnormal growth of cells inside the brain or central spinal vessels. Cell growth can be explained based on its origin and behavior in benign (non-cancerous) or malignant (cancerous) tumors. The categorization for a brain tumor has been formulated by the World Health Organization (WHO); it is graded from I to IV in which a tumor of grade I exposes the presence of the least malignant tumor of grade IV, uncovering the existence of the most aggressive tumor [1]. Primarily, it arises within the brain, and examples comprise meningiomas, gliomas, and pituitary adenomas. Secondary brain tumors (metastatic) have metastasized to the brain from other bodily regions, such as the lungs or breast [2]. Even though the precise etiology of several brain tumors remains unknown, specific inherited mutations, radiation contact, and ancestral records of brain tumors are documented as potential risk features [3]. The symptoms of a brain tumor vary depending on its size, type, and location within the brain. Commonly observed signs include headaches, mood changes, nausea, seizures, and visual disturbances [4]. For the diagnosis of brain tumors, magnetic resonance imaging (MRI) is the dominant modality, which provides comprehensive cerebral images that help in discovering the dimensions and position of tumors [5].

The associate editor coordinating the review of this manuscript and approving it for publication was Binit Lukose.

The key diagnostic device of magnetic resonance imaging (MRI) is used in neuroimaging. MRI captures comprehensive pictures of the brain's internal structures by employing the nuclear magnetic resonance principles without the requirement of ionizing radiation, differentiating it from other imaging practices like X-rays [6]. MRI's built-in capability to distinguish among the soft tissues makes it advisable to adapt to separate the healthy brain and pathological tumor tissues. For the identification and delineation of tumor boundaries, this high-contrast resolution is vital [7]. Beyond the basic MRI, functional MRI (fMRI) procedures can draw active brain sections, whereas diffusion tensor imaging (DTI) can map out white matter zones. These unconventional approaches suggest insights into tumor metabolism, vascularization, and its potential influence on neural pathways [8]. MRI comprehensive pictures are irreplaceable for neurosurgeons scheduling surgical involvements. After treatment, MRI works as a monitoring instrument, assessing treatment effectiveness and detecting possible tumor reappearance [9], [10], [11]. However, MRI encounters challenges. The procedure involves the patients persisting for a prolonged time, which motion artifacts can influence, and it may be contraindicated for patients with specific devices or implants.

In machine learning, transfer learning has appeared as a transformative method, mostly in circumstances where the data for the required task is limited or costly to attain. Through leveraging information from an associated source task, transfer learning can speed up the process of training and enhance the performance of the model [12]. Huge datasets like ImageNet have been utilized to train deep neural networks. All models that are pre-trained, already practiced at removing intricate characteristics from pictures, can be modified on reduced, domain-specific datasets, for instance, a scan of an MRI brain to attain vigorous performance with a smaller amount of data [13]. As a substitute for training models from scrap, the transfer learning approach permits the removal and transmission of high-level characteristics from pre-trained models. Then, these characteristics can be used for several tasks, such as from classification to regression [14]. Reducing computational resources and time is one of the key benefits of transfer learning. Through leveraging the models that are pre-existing and their acquired characteristics, the necessity of widespread training on huge datasets is reduced, which presents the approach mainly appropriate for medical imaging, wherever datasets are frequently scarce [15]. Regarding detecting MRI brain tumors, synthesizing a transfer learning approach with traditional MRI analysis embraces promising results. By employing the influence of pre-trained models and the precious info existing in MRI scans, there is a potential for noteworthy developments in the precision and efficiency of brain tumor classification. This paper evaluates and compares the effectiveness of various transfer learning models for MRI brain tumor classification, particularly under conditions with limited training data—a common challenge in clinical settings. By investigating models such as VGG16, ResNet-50, InceptionV3, and DenseNet-121 within the Transformative Transfer Learning (TTL) framework, the study aims to identify trade-offs between accuracy, computational efficiency, and generalizability. The goal is to provide insights into which models are best suited for practical deployment in medical imaging, enhancing diagnostic support for brain tumor detection while addressing real-world constraints on data and resources. This study aims to develop and evaluate the TTL model to improve the accuracy of MRI brain tumor detection. By leveraging pre-trained deep neural networks and refining them with transfer learning techniques, the study seeks to compare the TTL model's performance against traditional classification methods, demonstrating its potential to significantly improve diagnostic accuracy and efficiency in medical imaging.

This paper makes several key contributions to the field of medical imaging and brain tumor detection:

- We introduce the TTL model, which leverages pre-trained deep neural networks and refines them using transfer learning techniques tailored for MRI brain tumor classification.
- The study outlines a detailed preprocessing pipeline, including resizing, normalization, noise removal, and data augmentation, ensuring high-quality inputs for the deep learning models.
- We conducted extensive experiments to evaluate the TTL model's performance using accuracy, precision, recall, and F1-score metrics. Our results demonstrate that the TTL model significantly outperforms traditional methods, including thresholding, wavelet-based SVM, texture analysis, and K-means clustering.
- The paper provides valuable insights into the practical application of transfer learning in medical imaging, highlighting its rapid convergence, efficient use of limited data, and superior generalization capabilities.

The rest of the paper is organized so that the next section highlights the existing literature and studies, followed by methodology in section III. The results and experiments are discussed in section IV, and the paper is concluded in section V.

II. RELATED WORK

The MRI brain tumor classification field has witnessed substantial advancements, transitioning from traditional image processing techniques to sophisticated machine learning and deep learning approaches. This section presents an overview of conventional and modern methods in MRI brain tumor classification, focusing on recent studies and the evolution of technology in this domain.

A. CONVENTIONAL APPROACHES FOR CLASSIFICATION OF MRI BRAIN TUMOR

Before integrating deep learning, MRI brain tumor classification primarily relied on traditional machine learning methods and handcrafted feature extraction. These methods, while foundational, were limited by their dependence on manually engineered features and relatively simplistic algorithms.

Image segmentation was a core technique in these conventional approaches, dividing images into segments to identify tumor regions. Methods like thresholding, region-growing, and watershed algorithms were widely used to delineate tumor boundaries within MRI scans. While effective to some extent, these segmentation methods struggled with accuracy when dealing with complex tumor shapes or variations in intensity across image analysis. They have also played a key role in traditional classification, with features derived from intensity distributions that characterize tumor regions.

Techniques such as co-occurrence matrices, Gabor filters, and wavelet transforms were commonly applied to extract texture features, providing valuable information about the structural patterns of tumors [16]. Although they contributed significantly to early classification efforts, they faced challenges adapting to the variability in MRI data, often resulting in limited accuracy and generalizability [17]. Mean, variance, skewness, and kurtosis are statistical measures used to describe tumor features. They are based on the intensity values of MRI scans. Morphological image processing, which includes operations like expanding, contracting, opening, and closing, has been used to make brain tumors look better in MRI scans [18]. Usually, the features mentioned above were fed into traditional machine learning classifiers such as Support Vector Machines (SVM), Decision Trees, and K-nearest neighbors (KNN) to sort the tumors into groups.

B. APPLICATIONS OF DEEP LEARNING IN MEDICAL IMAGING

Deep learning, a subset of machine learning, has revolutionized the field of medical imaging in recent years. Deep learning models can automatically learn hierarchical representations from raw data using neural networks with multiple layers (deep architectures). This means that traditional methods don't need to be used to extract features manually [21]. Unlike traditional methods that rely on handcrafted features, deep learning models can automatically learn and extract relevant features from medical images [22]. With access to large datasets and powerful computing power, deep learning models have surpassed traditional methods in several medical imaging tasks, being the best at what they do [23]. MRI, x-rays, and ultrasounds are different imaging techniques that can be utilized by deep learning techniques to effectively predict the patient's health condition. However, it possesses its challenges when using deep learning with medical imaging [24]. These challenges include the size of the dataset, annotations from the experts, and the interpretability and understandability of these models. The integration of deep learning with medical imaging holds immense promise. It can enhance diagnostic accuracy, streamline workflows, and facilitate personalized patient care.

C. APPLICATIONS FOR TRANSFER LEARNING IN MEDICAL IMAGING

Transfer learning has quite a reasonable application in medical images. It has numerous benefits to the health sector due to the challenges associated with medical data. It is helpful when the data size is small, there is variability in the dataset, and fewer annotated images are available. The transfer learning learns the features from another dataset, evaluates the weight accordingly, and then utilizes those pre-trained values to tune it according to the new data [28]. In another study, transfer learning showed superior performance with a small dataset [29]. Transfer learning can also extract meaningful features from medical images using pre-trained models. These features can then be fed into traditional machine learning classifiers for diagnosis or other tasks [30]. In scenarios where the source and target domains differ significantly, domain adaptation techniques can be employed to bridge the gap, ensuring that the knowledge transfer is effective [31]. TABLE 1 presents the description of transfer learning in medical imaging.

TABLE 1. Notable works on transfer learning in medical imaging.

Ref.	Methodology	Medical Imaging Task	Key Findings
[29]	Fine-tuning of CNNs	Lesion detection in X-rays	Demonstrated the efficacy of transfer learning in detecting lesions with limited annotated data.
[30]	Feature extraction using pre-trained models	Diabetic retinopathy classification	Highlighted the potential of transfer learning in extracting robust features for retinal images.
[31]	Domain adaptation in transfer learning	Cross-modality brain tumor segmentation	Showed that domain adaptation can effectively bridge the gap between MRI and CT modalities.

Existing MRI brain tumor classification technologies often struggle with data scarcity, as medical datasets are typically limited and costly to annotate. Traditional machine learning methods require large, labeled datasets to achieve high accuracy, which is a significant limitation in medical imaging [32]. Additionally, these methods often demand substantial computational resources and time, particularly when training from scratch. The TTL model effectively addresses these challenges by leveraging transfer learning, utilizing pre-trained deep neural networks that can adapt to new, domain-specific tasks with minimal additional data. This approach reduces training time and computational load, as the model requires fewer resources and data to achieve high performance, making it a practical solution for medical applications with limited datasets. The exploration of transfer learning in medical imaging is still an active area of research, with ongoing studies aiming to optimize knowledge transfer further and improve model generalization across diverse medical imaging tasks.

III. METHODOLOGY

This section discusses the methods and materials used in this research. It explains the data collection process, description, pre-processing, and methodology. As shown in Figure 1,

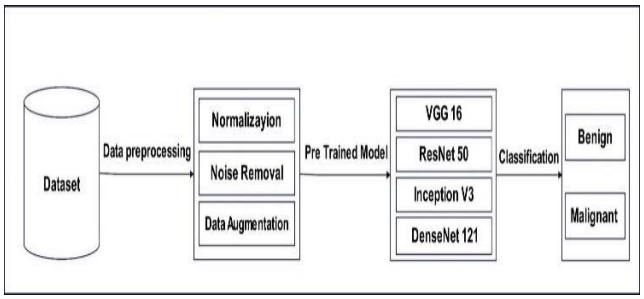

FIGURE 1. Proposed methodology of transfer learning-based tumor detection.

this section is divided into subsections according to the methodology phases.

A. DATA COLLECTION AND PREPROCESSING

The initial task of the dataset collection involves collecting data from multiple sources to ensure a diverse dataset. After the data collection, we performed a comprehensive set of preprocessing operations to make the dataset as clean as possible. The following are the preprocessing steps performed to refine the dataset.

As the dataset was collected from multiple sources, all the images were resized to the standard size, i.e. 256×256 pixels for a uniform format. Each MRI image III of arbitrary size is resized to a uniform size of 256×256 pixels.

$$I' = resize(I, 256, 256) \tag{1}$$

where I' is the resized image.

Normalization: All the values of the MRI were normalized to a range of 0 and 1. Each pixel value p in the MRI image is scaled to a range of [0, 1]. If the original pixel values are in the range $[p_{min}, p_{max}]$, normalization can be defined as:

$$p_{normalized} = \frac{p - p_{min}}{p_{max} - p_{min}} \tag{2}$$

This transforms the pixel intensity values of $p_{normalized}$ to fall between 0 and 1.

Noise removal: MRI scans are commonly pruned to the noise due to different factors. Thus, a Gaussian filter removes the random noise from the image. A Gaussian filter is applied to each MRI image to reduce random noise. The Gaussian filter G_σ is defined by:

$$G_\sigma\,(x, y) = \frac{1}{2\pi\sigma^2} e^{-\frac{x^2+y^2}{2\sigma^2}} \tag{3}$$

where σ is the standard deviation, controlling the extent of smoothing. The filtered image $I_{filtered}$ is obtained by convolving I with G_σ:

$$I_{filtered} = I * G_\sigma \tag{4}$$

Data Augmentation: To increase the dataset size and add more versatility, different augmentation techniques, i.e., rotation, flipping, and zooming, were applied. Various transformations are applied to increase the dataset size and variability. Let I be an image and T be a set of augmentation transformations, such as rotation, flipping, and zooming:

- **Rotation:**

$$I_{rotated} = rotate(I\theta) \tag{5}$$

where θ is the rotation angle in degrees, typically selected within a range (e.g., $-15°$ *to* $+15°$).

- **Zooming:**

$$I_{zoomed} = zoom(Iz) \tag{6}$$

where z is the zoom factor, usually within a range (e.g., 0.8 to 1.2).

- **Flipping:**

$$I_{flipped} = flip(I, horizontal/vertical) \tag{7}$$

1) MRI DATASET DESCRIPTION

In this research, the dataset used in the experiments and test is formed based on the Nickparvar brain MRI images dataset [31] and the Cheng brain tumor dataset [32]. The description of the dataset is presented in TABLE 2 and Figure 2. The dataset comprises 6,000 MRI scans, each serving as a distinct data point for analysis. Uniformity across the dataset is maintained with each scan presented at a resolution of 256×256 pixels, ensuring consistent quality and detail for image processing tasks. All scans are stored in the Digital Imaging and Communications in Medicine (DICOM) format, the standard protocol for managing and transmitting medical imaging information. The images include representations of various tumor types, specifically Glioma, Meningioma, and Pituitary tumors, providing a broad scope for the model to learn and identify these conditions. Out of the total scans, 3,500 are annotated as positive cases, indicating the presence of a tumor, which is pivotal for training the model to recognize pathological features. The dataset also includes 2,500 scans classified as negative cases where no tumor is present, which is essential for teaching the model to differentiate between pathological and normal anatomy. The data was divided into training, validation, and testing sets in an 80-10-10 split.

TABLE 2. MRI dataset overview.

Attribute	Description
Total Scans	6,000
Resolution	256x256 pixels
Format	DICOM
Types of Tumors	Glioma, Meningioma, Pituitary
Positive Cases	3,500 (Tumor present)
Negative Cases	2,500 (No tumor)

2) IMAGE AUGMENTATION TECHNIQUES

Due to several issues, medical dataset size is a challenge. Therefore, image augmentation is an integral part of most

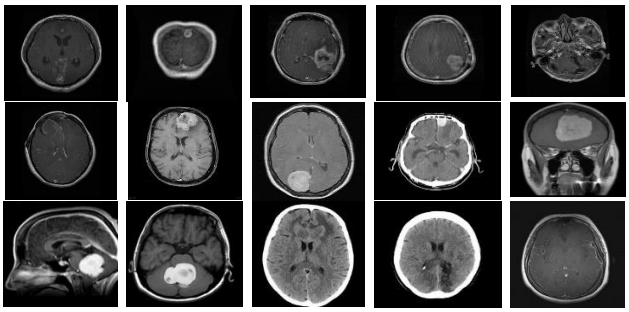

FIGURE 2. Sample MRI scans from the dataset.

deep-learning solutions. Data augmentation has many advantages besides the size increase. It can add variation to the dataset and help generalize the model. TABLE 3 presents the commonly used data augmentation techniques used in this research.

TABLE 3. Overview of image augmentation techniques.

Technique	Description	Use in MRI Scans
Rotation	Rotating the image by a certain angle	Introducing rotational variations
Flipping	Flipping the image horizontally or vertically	Exploiting brain hemisphere symmetry
Zooming	Zooming in or out of the image	Simulating distance variability
Brightness & Contrast Adjustment	Altering the image's brightness and contrast levels	Simulating intensity variations
Sharing	Skewing the image along an axis	Introducing perspective distortions
Elastic Deformation	Applying localized spatial transformations	Simulating organic structure variability

B. TRANSFER LEARNING

Transfer learning has emerged as a cornerstone in deep learning, particularly when confronted with limited datasets. Transfer learning lets you take learned features and use them on new, related tasks using models already trained on huge datasets. This approach accelerates the training process and often results in enhanced model performance, especially in domains like medical imaging, where annotated data can be scarce.

1) PRE-TRAINED MODELS

This section explores the methodology behind leveraging transfer learning capabilities for specific tasks, emphasizing its sequential architecture that captures complex image features through deep hierarchical processing. The base models for transfer learning are VGG16, ResNet 50, InceptionV3, and DenseNet-121.

VGG16, a convolutional neural network (CNN) architecture, is often used as a base model for transfer learning due to its simplicity and effectiveness. This section describes the methodology of applying VGG16 transfer learning for our specific task.

VGG16 is characterized by its deep architecture consisting of 16 convolutional and fully connected layers. It follows a sequential structure, with alternating convolutional and max-pooling layers, followed by fully connected layers. The architecture is designed to capture the hierarchical features of images through progressively deeper layers, as shown in Figure 3.

$$O_{i,j}^{(l)} = \sigma\Big(\sum_{m=1}^{M^{(l-1)}} \sum_{n=1}^{N^{(l-1)}} \sum_{k=1}^{K^{(1)}} W_{m,n,k}^{(l)} . I_{i+m-1,j+n-1}^{(l-1)} + b_k^{(l)}\Big) \tag{8}$$

where $O_{i,j}^{(l)}$ is the output activation at position (i,j)in layer l, σ is the activation function (e.g., ReLU), $W_{m,n,k}^{(l)}$ is the weight of the k-th filter at position (m, n) in the layer l, $\mathrm{I}_{i,j}^{(l-1)}$ is the activation at position (I, j) in the previous layer l-1, $\mathrm{b}_k^{(l)}$ is the bias term for the k-th filter, $\mathrm{M}^{(l-1)}$ and $\mathrm{N}^{(l-1)}$ are the spatial dimensions of the previous layer's activations, $\mathrm{K}^{(l)}$ is the number of filters in layer l.

$$O_{i,j}^{(l)} = \max_{m,n}(\mathrm{I}_{2i+m,2j+n}^{(l-1)}) \tag{9}$$

where $O_{i,j}^{(l)}$ is the output activation at position (i, j) in layer l, and $\mathrm{I}_{i,j}^{(l-1)}$ is the activation at position (i, j) in the previous layer $\mathrm{l} - 1$.

$$O_k^{(l)} = \sigma\Big(\sum_{j=1}^{j^{(l-1)}} W_{j,k}^{(L)} . I_j^{(l-1)} + b_k^{(l)}\Big) \tag{10}$$

where $\mathrm{O}_k^{(l)}$ is the output neuron at position k in layer l, $\mathrm{W}_{j,k}^{(L)}$ is the weight connecting the j^{th} neuron in the previous layer to the k^{th} neuron in layer l, $\mathrm{I}_j^{(l-1)}$ is the activation of the j^{th} neuron in the previous layer, $\mathrm{b}_k^{(l)}$ is the bias term for the k^{th} neuron, $\mathrm{J}^{(l-1)}$ is the number of neurons in the previous layer.

$$W \leftarrow W - \eta \frac{\partial L}{\partial W}$$
$$B \leftarrow b - \eta \frac{\partial L}{\partial b} \tag{11}$$

where η is the learning rate, $\frac{\partial L}{\partial W}$ and $\frac{\partial L}{\partial b}$ are the gradients of the loss function concerning the weights and biases, respectively.

ResNet-50 is a convolutional neural network architecture, as shown in Figure 4ResNet-50 is characterized by residual blocks, which enable the training of intense neural networks while mitigating the vanishing gradient problem. It consists of 50 layers and has shown outstanding performance in various computer vision tasks, including image classification.

InceptionV3 is a CNN architecture developed by Google. It is renowned for its deep architecture and efficient use of computational resources. InceptionV3 employs the Inception module, allowing the network to capture features at multiple spatial scales efficiently.

$$O_{concat} = concat(C_{1\times1}, C_{3\times3_{reduce}}, C_{3\times3}, \times C_{5\times5\_reduce}, C_{5\times5}, C_{pool\_proj}) \tag{12}$$

where O_{concat} is the concatenated output, $C_{1\times1}$, $C_{3\times3_{reduce}}$, $C_{3\times3}$, $C_{5\times5\_reduce}$, $C_{5\times5}$, C_{pool_proj} represent the outputs of different convolutional operations within the Inception module.

$$sO_k = \frac{1}{H \times W} \sum_{i=1}^{H} \sum_{j=1}^{W} I_{i,j,k} \tag{13}$$

where O_k is the output feature for the k^{th} channel, H and W are the height and width of the feature map, respectively, $I_{i,j,k}$ is the activation at position (ij) for the k^{th} channel.

$$W_{new} \leftarrow W_{pre-trained} - \eta \frac{\partial L}{\partial W\ new}$$
$$b_{new} \leftarrow b_{pre-trained} - \eta \frac{\partial L}{\partial b\ new} \tag{14}$$

where W_{new} and b_{new} are the weights and biases of the new classification layer, $W_{pre-trained}$ and $b_{pre-trained}$ are the pre-trained weights and biases, η is the learning rate, $\frac{\partial L}{\partial W\ new}$ and $\frac{\partial L}{\partial b\ new}$ are the gradients of the loss function L concerning the new weights and biases, respectively.

DenseNet-121 consists of multiple dense blocks, as shown in Figure 5, each containing several dense layers, followed by transition layers to reduce the spatial dimensions. The dense connectivity pattern facilitates feature reuse and gradient flow throughout the network, improving parameter efficiency and feature propagation.

$$H_l = concat(H_1, H_2, \ldots, H_{l-1}) \tag{15}$$

where H_l is the output feature map of the layer l, H_i represents the feature maps of all preceding layers up to i, concat denotes the concatenation operation.

$$H_l = ReLU(BN\ (H_{l-1}) * W_l) \tag{16}$$

where H_{l-1} is the input feature map, $*$ denotes the convolution operation, W_l represents the weights of the convolutional filters, BN denotes batch normalization, and ReLU is the rectified linear unit activation function.

$$H_l = AvgPool(\mathrm{BN}\ (ReLU\ (H_{l-1}) \times 1 \times 1)) \tag{17}$$

where AvgPool denotes the average pooling operation, $^*1 \times 1$ represents a 1×1 convolutional operation.

Several deep learning architectures have been pre-trained on large datasets, like ImageNet, which contains millions of images spanning thousands of categories. Each network was chosen based on its ability to provide unique strengths that contribute to effective MRI brain tumor classification. VGG16's simplicity, ResNet-50's depth and resilience to gradient issues, InceptionV3's multi-scale approach, and DenseNet-121's feature reuse and parameter efficiency each offer distinct advantages that, when combined through transfer learning, provide robust performance on complex medical images. This combination enables the TTL model

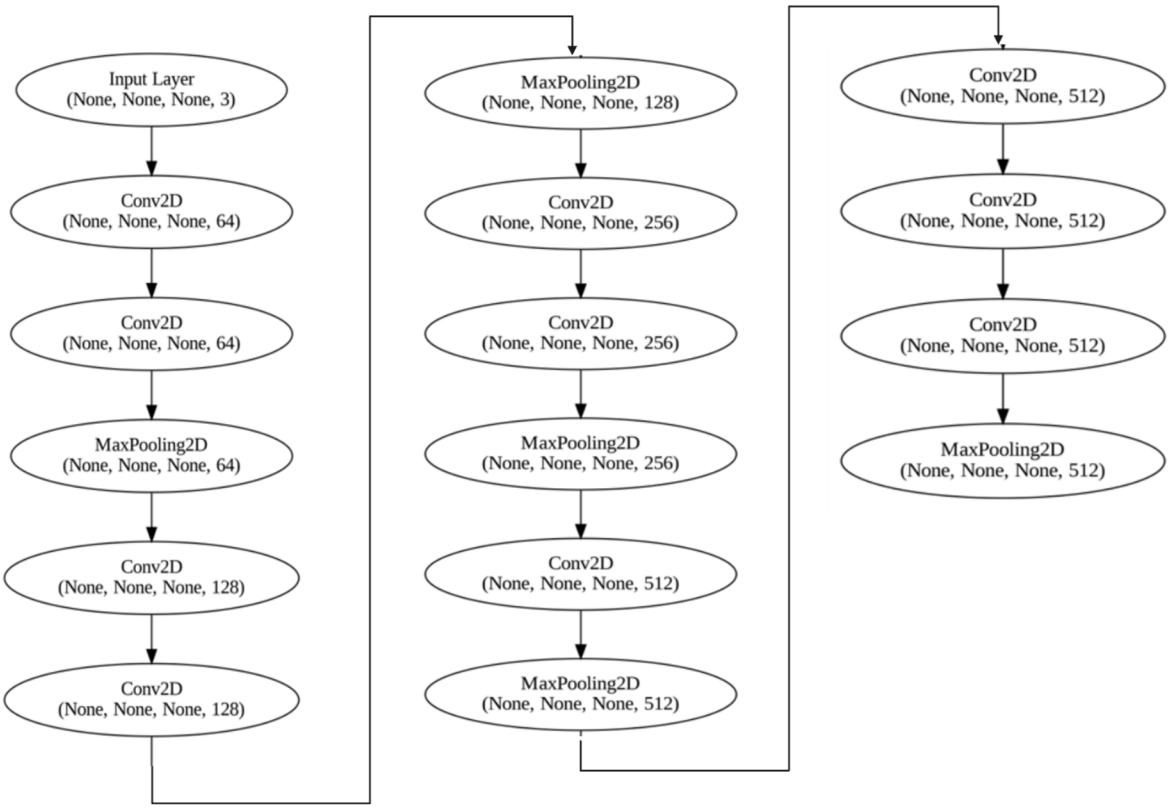

FIGURE 3. VGG16 model architecture.

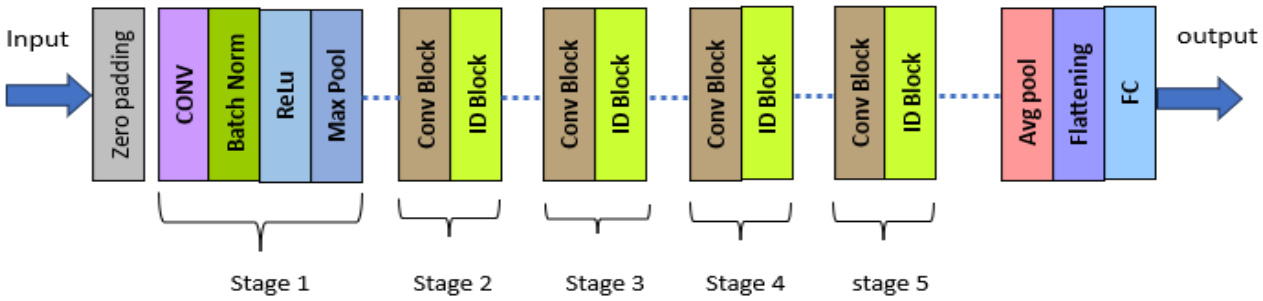

FIGURE 4. Resnet-50 Model architecture.

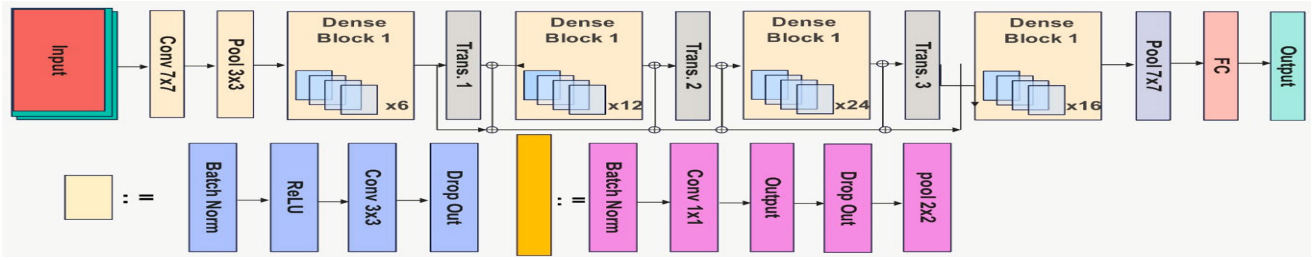

FIGURE 5. DenseNet-121.

to maximize classification accuracy while managing data limitations and computational demands typically encountered in medical imaging applications.

These models, having learned a plethora of features from diverse images, can be fine-tuned or adapted for specific tasks in medical imaging, as shown in TABLE 4.

TABLE 4. Overview of pre-trained models used in medical imaging.

Model Name	Dataset	Key Features	Typical Use in Medical Imaging
VGG16	ImageNet	16 layers (13 convolutional), ReLU activation, Max pooling	Tumor classification, Lesion detection
ResNet-50	ImageNet	50 layers, Residual connections, Batch normalization	Image segmentation, Disease classification
InceptionV3	ImageNet	Multiple kernel sizes, Concatenated outputs, Global average pooling	Anomaly detection, Image classification
DenseNet-121	ImageNet	121 layers, Dense connections between layers, Growth rate parameter	Radiograph analysis, Tumor segmentation

2) FINE-TUNING STRATEGIES

The next key step in transfer learning is parameter fine-tuning. The fine-tuning of parameters refined the model according to the new application area and dataset requirement. This task ensures that the model uses the existing knowledge learned from the previous dataset and extracts and refines the knowledge learned from the new dataset. There are different strategies for model tuning, which are summarized in TABLE 5.

TABLE 5. Overview of fine-tuning strategies.

Strategy Name	Description	When to Use	Potential Benefits
Full Model Fine-tuning	Fine-tuning all layers of the pre-trained model	Large new dataset; Significant differences from the original dataset	Comprehensive adaptation to new data
Partial Fine-tuning	Fine-tuning only the top layers, freezing the bottom ones	Small new dataset; Risk of overfitting	Retains foundational features; Reduces overfitting
Feature Extraction & Retraining	Extracting features and training a new classifier	When wanting to keep the pre-trained model unchanged	Flexibility: Utilizes pre-trained knowledge
Learning Rate Scheduling	Using a dynamic learning rate during fine-tuning	Any fine-tuning scenario	Balances retention of old knowledge with new learning

Figure 6 shows the graphical representation of the model tuning process. It highlights that some parts remain unchanged, as shown in grey shades. However, the green part can change according to the new dataset and environment. The hyperparameter configuration for the proposed model was optimized to achieve robust performance on MRI brain tumor classification. Key settings included a learning rate

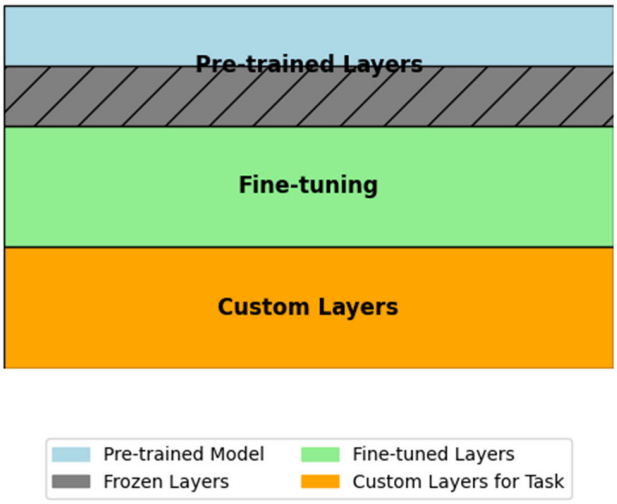

FIGURE 6. Fine-tuning process visualization.

of 0.001 with a decay schedule to ensure gradual adjustments during training and a batch size of 32 to balance computational efficiency with model stability. Due to its adaptive learning capabilities, we employed the Adam optimizer, setting dropout rates at 0.5 to reduce overfitting. The model was trained for 50 epochs, with early stopping based on validation loss to prevent excessive training. This configuration was selected after preliminary tuning experiments to optimize accuracy, convergence, and generalization.

C. MODEL EVALUATION METRICS

Evaluating a model's performance is crucial in determining its efficacy and reliability. Several metrics can be employed to assess different aspects of a model's predictions, especially in medical imaging, where precision is paramount. No single performance metric evaluates all the dimensions of the classification and prediction models. Therefore, this research uses the following metrics to perform a multi-dimensional model evaluation.

Accuracy: This general metric calculates the proportion of all correct predictions over the total predictions made.

$$Accuracy = \frac{\mathrm{TP} + \mathrm{TN}}{\mathrm{TP} + \mathrm{FP} + \mathrm{TN} + \mathrm{FN}} \tag{18}$$

Precision: Precision, also known as the positive predictive value, measures the proportion of true positive predictions among all positive predictions made by the model.

$$Precision = \frac{\mathrm{TP} + \mathrm{FP}}{\mathrm{TP}} \tag{19}$$

Recall (sensitivity): Recall calculates the proportion of true positive predictions and overall actual positive instances in the dataset.

$$Recall = \frac{\mathrm{TP} + \mathrm{FN}}{\mathrm{TP}} \tag{20}$$

Specificity: This metric measures the proportion of true negative predictions and overall actual negative instances in the dataset.

$$Specificity = \frac{\mathrm{TN}}{\mathrm{TN} + \mathrm{FP}} \tag{21}$$

F1-Score: The F1-score is the harmonic means of precision and recall, balancing the two when there's an uneven class distribution.

$$\mathrm{F1} = 2\frac{Precision \times \mathrm{Recall}}{Precision + \mathrm{Recall}} \tag{22}$$

AUC-ROC: The ROC curve plots recall against the 1-specificity for different threshold values. The perfect score for AUC is 1, which means the model is 100% correct, while 0 refers to 0 % accuracy.

IV. IMPLEMENTATION

The next step is implementing the model. This section explains the implementation process, which includes the environmental setup, data loading, and augmentation.

A. EXPERIMENTAL ENVIRONMENT

The experiments were carried out on the Google Colab with Python 3 environment. The default GPU session was used. The RAM and hard disk are utilized with standard computing. The coding is based on the TensorFlow and Keras frameworks.

B. DATA LOADING AND AUGMENTATION

Once the environment was set up, the focus shifted to data handling. The Pydicom library was used to load the dataset in DICOM format. Then, data augmentation techniques are applied to implement zooming, rotation, and flipping. The details are presented in TABLE 6.

TABLE 6. Data augmentation techniques and libraries.

Augmentation Technique	Description	Library/Tool Used
Rotation	Rotating the image by a certain angle	ImageDataGenerator (Keras)
Flipping	Flipping the image horizontally or vertically	ImageDataGenerator (Keras)
Zooming	Zooming in or out of the image	ImageDataGenerator (Keras)
Brightness & Contrast Adjustment	Altering the image's brightness and contrast levels	augmenters (imgaug)

C. MODEL ARCHITECTURE AND ADAPTATION

The MRI dataset has two main challenges: first, it contains very complex information, and second, the nature of the tumor is critical in terms of its size, position, and type. Therefore, ResNet-50 was selected as a base model for this study. The deep layers and their residual connections are advantageous for extracting information from complex images like MRI.

The pre-trained model of ResNet-50 is then refined as follows. The top layers are discarded to adapt to the MRI dataset. A dense and pooling layer with a sigmoid function

predicts the tumor classes. The Adam optimizer is selected as an optimization function, while several evaluation metrics are used to evaluate the binary class prediction.

Next, the dataset was split into training, validation, and test sets with 80, 10, and 10 ratios. The batch size was set to 32, and the model was trained for 50 epochs. These parameters were selected based on preliminary experiments to balance training speed and model performance. The initial loss is presented in Figure 7.

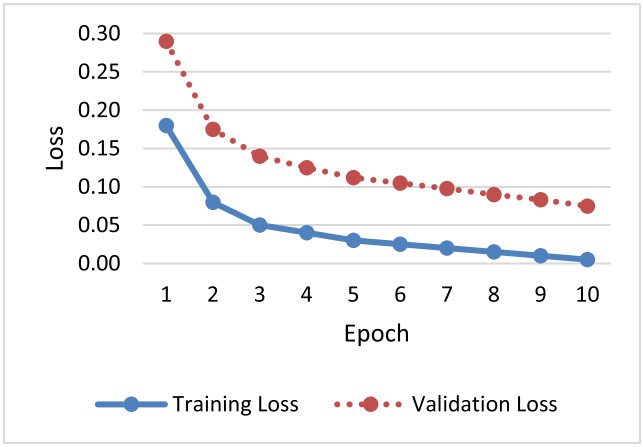

FIGURE 7. Model training and validation loss curves.

V. RESULTS AND DISCUSSION

This section presents the results and discusses the experiments. It evaluates the detailed performance of the applied models on the dataset and its outcomes.

A. MODEL PERFORMANCE ON TEST DATA

This section presented the results of the model performance on the test dataset. The results revealed very promising results. The results indicated a very highly accurate prediction with 94.5% accuracy. Similarly, the model can predict most tumor cases positively and yield a 93.2% precision rate. In addition, the reported recall was 92.8 %, which shows the identification of the actual positive cases. To check the harmonic mean of the precision and recall, the f1 measure is reported, which stood at 93%, an auspicious result. These results are summarized in TABLE 7.

TABLE 7. Model performance metrics on test data.

Metric	Value (%)
Accuracy	94.5
Precision	93.2
Recall	92.8
F1-Score	93.0

B. COMPARISON WITH STATE-OF-THE-ART

The experiments show auspicious results for the deep learning-based model. This section compares the proposed model's results with those of traditional models. The comparison is provided with existing models, including threshold-based image segmentation, wavelet-based feature extraction, texture-based model, and clustering-based predictions.

While deep learning and transfer learning have shown significant promise in medical imaging tasks, it's essential to juxtapose their performance against traditional image processing and machine learning methods. This comparison provides a holistic view of the advances made and the potential areas for improvement. The results in TABLE 8, the deep learning-based model outperformed the traditional models in all four dimensions. Wavelet with SVM is the second method that performed better. The good performance is due to the model's ability to extract complex information from the MRI image using different layers and parameter-tuning strategies.

TABLE 8. Performance comparison of deep learning model with traditional methods.

Method	Accuracy (%)	Precision (%)	Recall (%)	F1-Score (%)
Deep Learning (Transfer Learning)	**94.5**	**93.2**	**92.8**	**93.0**
Thresholding	78.6	76.1	80.2	78.1
Wavelets + SVM	82.3	81.7	83.0	82.3
Texture Analysis	80.4	79.9	81.1	80.5
K-means Clustering	77.2	75.8	78.6	77.2

Figure 8 visually contrasts the performance of the deep learning model with traditional methods. The superior performance of the deep learning model, especially in terms of accuracy and F1 score, is evident.

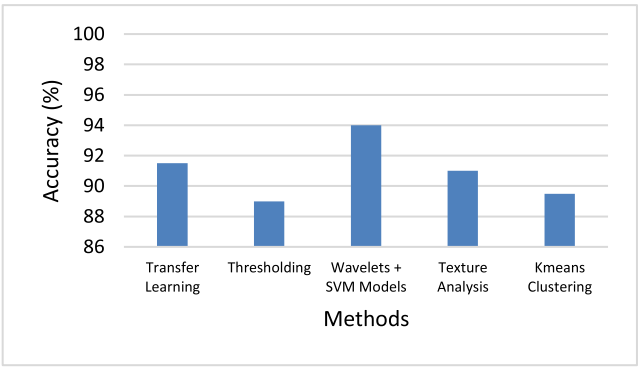

FIGURE 8. Model performances.

The results highlight the advantages of leveraging deep learning for MRI brain tumor classification, particularly transfer learning. While traditional methods have their merits and have been foundational in the field, the deep learning model outperforms them across all metrics. The ability of deep learning models to automatically learn features from data rather than relying on manually crafted features likely contributes to their superior performance. However, it's also crucial to acknowledge that deep learning models

require more computational resources and data than traditional methods. As technology advances and datasets grow, the performance gap is expected to widen further in favor of deep learning.

C. INSIGHTS FROM TRANSFER LEARNING

As a framework, transfer learning has fundamentally transformed the methodology of training deep learning models, particularly in fields where data may be limited or costly to acquire, like medical imaging. The subsequent points are fundamental observations obtained by utilizing transfer learning to categorize brain tumors in MRI scans:

An initial benefit that was noted is the rapidity of convergence. Models initialized with weights from pre-trained networks exhibited faster convergence than those with random weights. This is because pre-trained models have already acquired a substantial feature representation from their original datasets, which are typically extensive and varied.

Transfer learning has shown its effectiveness in situations with a shortage of labeled data. Despite the reduced dataset, the model achieved impressive performance, highlighting the technique's efficient data utilization.

Transfer learning-trained models demonstrated superior generalization on unfamiliar data. This is due to the rich feature representations acquired from extensive datasets such as ImageNet, which encompass diverse patterns and structures.

Mitigation of Overfitting: Utilizing transfer learning, particularly by fine-tuning only the top layers of a model, can effectively reduce the probability of overfitting. This is because the lower layers, which are in a fixed state, possess more generalized characteristics with a lesser probability of excessively fitting to the training data.

The adaptability of transfer learning was seen. Although the pre-trained models were first trained on natural images, they can be successfully adapted for medical imaging applications, demonstrating the general applicability of certain learned properties.

Figure 9 indicates the features identified by the pre-trained model while analyzing MRI scans. The recorded patterns emphasize the extensive and comprehensive knowledge transmitted from that initial dataset.

The knowledge obtained by transfer learning reinforces its ability to bring about significant changes in deep learning. Transfer learning overcomes the limitation of relying solely on data from one domain by utilizing knowledge from another area. This allows for achieving high performance even with limited resources. Transfer learning is beneficial for crucial applications like medical imaging, where the outcome of each prediction carries substantial ramifications. The resilience and reliability provided by transfer learning are highly advantageous in these scenarios.

A portion of the MRI dataset was isolated, especially annotated for Glioblastoma. Subsequently, the model was assigned the responsibility of categorizing these images, and its prognostications were juxtaposed with the verifiable

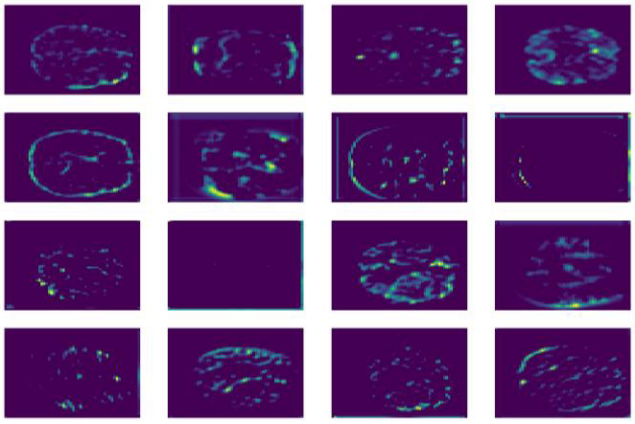

FIGURE 9. Feature visualization from transfer learning.

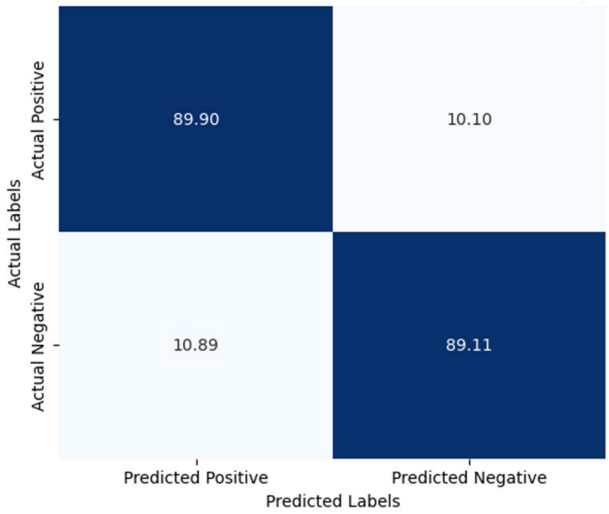

FIGURE 10. Confusion matrix for glioblastoma detection.

comments provided by radiologists. The model accurately classified 92 MRI scans as glioblastoma. There were eight instances where MRI images were mistakenly categorized as glioblastoma. A total of 85 MRI scans were accurately classified as non-glioblastoma. The program failed to detect and classify 15 MRI scans as glioblastoma. The numerical data is consolidated in TABLE 9.

TABLE 9. Glioblastoma detection results.

Metric	Value
True Positives	92
False Positives	8
True Negatives	85
False Negatives	15

Figure 10 illustrates the model's predictions for detecting glioblastoma. The comparison between forecasts and the actual data emphasizes the model's advantages and areas for improvement.

The case study highlights the model's capacity to identify glioblastoma, which is crucial considering the malignant characteristics of this tumor. Although the results show promise, false negatives highlight areas that need to be enhanced. The failure to recognize glioblastoma can have substantial clinical consequences. Subsequent versions of the model can prioritize minimizing these errors by integrating additional domain-specific information or improving the training procedure.

D. MENINGIOMA CLASSIFICATION

Meningiomas are tumors originating from the meninges, the tissue layers surrounding the brain and spinal cord. Although most meningiomas are not malignant, they can differ in terms of their growth rate and likelihood of recurring. Accurate classification of them is vital for

choosing a suitable therapeutic approach. A distinct subset of the MRI dataset was isolated, specifically annotated for meningiomas. Subsequently, the model was responsible for categorizing these photos into possible classifications: 'Benign Meningioma,' 'Atypical Meningioma,' and 'No Meningioma.' The model accurately classified 105 MRI scans as benign meningiomas, while it incorrectly classified 10 scans. Out of 70 MRI images, all were accurately identified as atypical meningiomas, whereas seven scans were incorrectly diagnosed. Out of the 95 MRI scans, it was accurately determined that they showed no 1igns of meningioma. However, eight images were mistakenly categorized as having meningioma. The results are presented in TABLE 10.

TABLE 10. Meningioma classification result.

Category	Correctly Classified	Misclassified
Benign Meningioma	105	10
Atypical Meningioma	70	7
No Meningioma	95	8

The case study showcases the model's capacity to not only identify the existence of a meningioma but also categorize its specific subtype. The high level of detail in classification can be quite beneficial in clinical settings, guiding treatment decisions. Although the results are promising, the misclassifications underscore the necessity for additional improvement. Including additional data, particularly for atypical meningiomas, would be beneficial, and domain-specific expertise may be incorporated to improve the model's accuracy in future iterations.

E. PITUITARY TUMOR IDENTIFICATION

The pituitary gland, the ''primary gland,'' is crucial in controlling multiple physiological processes. Pituitary gland tumors, although predominantly not malignant, may affect their function and result in a wide range of health issues. Precise identification of malignant malignancies is crucial for prompt action and therapy.

A specialized subset of the MRI dataset, specially annotated for pituitary tumors, was employed. Subsequently, the model was assigned to categorizing these images, and its forecasts were compared to the accurate annotations provided by proficient radiologists.

The case study highlights the model's capacity to detect pituitary tumors precisely. Early and precise diagnosis of tumors is crucial due to the pivotal function of the pituitary gland in the human body. The results exhibit promise; however, false negatives draw attention to certain areas that necessitate more consideration, as indicated in Figure 10. Exploring methods to increase the model's sensitivity, such as including additional training data or refining the architecture, could be possible areas of future investigation.

TABLE 11. Comparative analysis of proposed TTL model with state-of-the-art algorithms for MRI brain tumor classification.

Algorithm	Accuracy (%)	Precision (%)	Recall (%)	F1-Score (%)
Proposed TTL Model	94.5	93.2	92.8	93.0
Thresholding[17]	78.6	76.1	80.2	78.1
Wavelet-Based SVM [33]	82.3	81.7	83.0	82.3
Texture Analysis[16]	80.4	79.9	81.1	80.5
K-Means Clustering [34]	77.2	75.8	78.6	77.2

Table 11 demonstrates the comparative advantage of our proposed TTL model, which achieves higher performance across all metrics compared to traditional algorithms, underscoring the effectiveness of transfer learning in enhancing classification accuracy and robustness in MRI brain tumor detection.

VI. CONCLUSION AND FUTURE WORK

In conclusion, research into transfer learning for classifying MRI brain tumors provides crucial new information about the technology's possible uses in the medical imaging industry. The study revealed the excellent performance of deep learning models in accurately diagnosing brain cancers, surpassing previous methods. The model's high accuracy has significant implications for clinical practice, providing valuable support to radiologists. Additionally, it has the potential to expedite diagnostic processes, resulting in faster treatment decisions and cost savings. Furthermore, the prompt and precise identification enabled by these models shows the potential for enhancing patient results and overall quality of life.

Future research should enhance the interpretability of deep learning models, improve generalizability by expanding datasets, explore advanced neural network architectures, conduct real-world testing to assess practical utility, and address ethical considerations. These recommendations emphasize the importance of adopting a thorough strategy to effectively incorporate automated diagnostic technology into clinical

practice while maintaining ethical standards and protecting patient privacy. The upcoming journey presents prospects for transforming patient care by combining medicine and technology.

For future work, it is important to focus on enhancing clinicians' comprehension of model predictions, integrating varied datasets, investigating advanced neural network structures, conducting practical testing, and addressing ethical concerns for responsible integration into healthcare practices. This multifaceted approach ensures the continued progress of transfer learning-driven models in medical imaging, promising a transformative impact on patient care at the intersection of medicine and technology.

DATA AVAILABILITY

The datasets used in this study are available publicly at [31] and [32]. However, the code will be made available to the corresponding author upon request.

CONFLICTS OF INTEREST

The authors declare no conflicts of interest.

REFERENCES

[1] D. N. Louis, A. Perry, G. Reifenberger, A. von Deimling, D. Figarella-Branger, W. K. Cavenee, H. Ohgaki, O. D. Wiestler, P. Kleihues, and D. W. Ellison, "The 2016 world health organization classification of tumors of the central nervous system: A summary," *Acta Neuropathologica*, vol. 131, no. 6, pp. 803–820, Jun. 2016.

[2] Y.-J. Cheng, F. Fan, Z. Zhang, and H.-J. Zhang, "Lipid metabolism in malignant tumor brain metastasis: Reprogramming and therapeutic potential," *Expert Opinion Therapeutic Targets*, vol. 27, no. 9, pp. 861–878, Sep. 2023.

[3] Q. T. Ostrom, H. Gittleman, G. Truitt, A. L. Boscia, C. Kruchko, and J. S. Barnholtz-Sloan, "CBTRUS statistical report: Primary brain and other central nervous system tumors diagnosed in the United States in 2011–2015," *Neuro-Oncology*, vol. 20, no. 4, pp. 1–86, Sep. 2018.

[4] K. Morrow, A. Sloan, J. J. Olson, and D. R. Ormond, "Congress of neurological surgeons systematic review and evidence-based guidelines on the management of recurrent diffuse low-grade glioma: Update," *J. Neuro-Oncology*, vol. 171, no. 1, pp. 105–130, Jan. 2025, doi: 10.1007/s11060-024-04838-5.

[5] P. Carpentieri-Primo, L. Nahoum, L. Almeida, F. Nacur, S. F. A. Júnior, and N. Ventura, "The dark side of T2: Central nervous system lesions with low signal intensity on T2-weighted imaging," *Radiologia Brasileira*, vol. 57, May 2024, Art. no. 20230085.

[6] K. Thomas, A. Fotaki, R. M. Botnar, and V. M. Ferreira, "Imaging methods: Magnetic resonance imaging," *Circulation, Cardiovascular Imag.*, vol. 16, no. 1, Jan. 2023, Art. no. 014068.

[7] Z. Chen, K. Pawar, M. Ekanayake, C. Pain, S. Zhong, and G. F. Egan, "Deep learning for image enhancement and correction in magnetic resonance imaging—State-of-the-art and challenges," *J. Digit. Imag.*, vol. 36, no. 1, pp. 204–230, Nov. 2022.

[8] G. Melchiorre, F. Giustiniano, S. Rathore, and G. Pileio, "Singlet-assisted diffusion-NMR (SAD-NMR): Extending the scope of diffusion tensor imaging via singlet NMR," *Frontiers Chem.*, vol. 11, Aug. 2023, Art. no. 1224336.

[9] J. Boto, R. Guatta, A. Fitsiori, J. Hofmeister, T. R. Meling, and M. I. Vargas, "Is contrast medium really needed for follow-up MRI of untreated intracranial meningiomas?" *Amer. J. Neuroradiol.*, vol. 42, no. 8, pp. 1421–1428, Aug. 2021.

[10] F. Ullah, M. Nadeem, M. Abrar, M. Al-Razgan, T. Alfakih, F. Amin, and A. Salam, "Brain tumor segmentation from MRI images using handcrafted convolutional neural network," *Diagnostics*, vol. 13, no. 16, p. 2650, Aug. 2023.

[11] I. J. H. G. Wamelink, A. Azizova, T. C. Booth, H. J. M. M. Mutsaerts, A. Ogunleye, K. Mankad, J. Petr, F. Barkhof, and V. C. Keil, "Brain tumor imaging without gadolinium-based contrast agents: Feasible or fantasy?" *Radiology*, vol. 310, no. 2, Feb. 2024, Art. no. e230793.

[12] E. Singh and N. Pillay, "A study of transfer learning in an ant-based generation construction hyper-heuristic," in *Proc. IEEE Congr. Evol. Comput. (CEC)*, Jul. 2022, pp. 1–7.

[13] J. Yosinski, J. Clune, Y. Bengio, and H. Lipson, "How transferable are features in deep neural networks," in *Proc. Adv. Neural Inf. Process. Syst.*, vol. 27, Dec. 2014, pp. 3320–3328.

[14] M. Oquab, L. Bottou, I. Laptev, and J. Sivic, "Learning and transferring mid-level image representations using convolutional neural networks," in *Proc. IEEE Conf. Comput. Vis. Pattern Recognit.*, Jun. 2014, pp. 1717–1724.

[15] C. Tan, F. Sun, T. Kong, W. Zhang, C. Yang, and C. Liu, "A survey on deep transfer learning," in *Proc. 27th Int. Conf. Artif. Neural Netw. (ICANN)*, Rhodes, Greece. Cham, Switzerland: Springer, Jan. 2018, pp. 270–279.

[16] E. S. Biratu, F. Schwenker, T. G. Debelee, S. R. Kebede, W. G. Negera, and H. T. Molla, "Enhanced region growing for brain tumor MR image segmentation," *J. Imag.*, vol. 7, no. 2, p. 22, Feb. 2021.

[17] Ali. M. Hasan, F. Meziane, and H. A. Jalab, "Performance of grey level statistic features versus Gabor wavelet for screening MRI brain tumors: A comparative study," in *Proc. 6th Int. Conf. Inf. Commun. Manage. (ICICM)*, Oct. 2016, pp. 136–140.

[18] J. P. Serra, *Image Analysis and Mathematical Morphology*, Illustrated, Reprint ed., London, U.K.: Academic, 1982, p. 411.

[19] G. M. N. R. Gajanayake, R. D. Yapa, and B. Hewawithana, "Comparison of standard image segmentation methods for segmentation of brain tumors from 2D MR images," in *Proc. Int. Conf. Ind. Inf. Syst. (ICIIS)*, Dec. 2009, pp. 301–305.

[20] S. Chicklore, V. Goh, M. Siddique, A. Roy, P. K. Marsden, and G. J. R. Cook, "Quantifying tumour heterogeneity in 18F-FDG PET/CT imaging by texture analysis," *Eur. J. Nucl. Med. Mol. Imag.*, vol. 40, no. 1, pp. 133–140, Jan. 2013.

[21] F. Ullah, A. Salam, M. Abrar, M. Ahmad, F. Ullah, A. Khan, A. Alharbi, and W. Alosaimi, "Machine health surveillance system by using deep learning sparse autoencoder," *Soft Comput.*, vol. 26, no. 16, pp. 7737–7750, Aug. 2022.

[22] T. Liu, E. Siegel, and D. Shen, "Deep learning and medical image analysis for COVID-19 diagnosis and prediction," *Annu. Rev. Biomed. Eng.*, vol. 24, no. 1, pp. 179–201, Jun. 2022.

[23] F. Ullah, A. Salam, M. Abrar, and F. Amin, "Brain tumor segmentation using a patch-based convolutional neural network: A big data analysis approach," *Mathematics*, vol. 11, no. 7, p. 1635, Mar. 2023.

[24] J. Ker, L. Wang, J. Rao, and T. Lim, "Deep learning applications in medical image analysis," *IEEE Access*, vol. 6, pp. 9375–9389, 2018.

[25] A. Krizhevsky, I. Sutskever, and G. E. Hinton, "ImageNet classification with deep convolutional neural networks," *Commun. ACM*, vol. 60, no. 6, pp. 84–90, May 2017.

[26] S. Hochreiter and J. Schmidhuber, "Long short-term memory," *Neural Comput.*, vol. 9, no. 8, pp. 1735–1780, Nov. 1997.

[27] Y. Midoh and K. Nakamae, "Image quality enhancement of a CD-SEM image using conditional generative adversarial networks," *Proc. SPIE*, vol. 10959, pp. 37–46, Mar. 2019.

[28] F. Ullah, M. Nadeem, M. Abrar, F. Amin, A. Salam, and S. Khan, "Enhancing brain tumor segmentation accuracy through scalable federated learning with advanced data privacy and security measures," *Mathematics*, vol. 11, no. 19, p. 4189, Oct. 2023. [Online]. Available: https://www.mdpi.com/2227-7390/11/19/4189

[29] N. Tajbakhsh, J. Y. Shin, S. R. Gurudu, R. T. Hurst, C. B. Kendall, M. B. Gotway, and J. Liang, "Convolutional neural networks for medical image analysis: Full training or fine tuning?" *IEEE Trans. Med. Imag.*, vol. 35, no. 5, pp. 1299–1312, May 2016.

[30] L. Peng, H. Liang, G. Luo, T. Li, and J. Sun, "Rethinking transfer learning for medical image classification," *medRxiv*, vol. 11, no. 26, Nov. 2022, Art. no. 22282782.

[31] W. Zhang, R. Li, H. Deng, L. Wang, W. Lin, S. Ji, and D. Shen, "Deep convolutional neural networks for multi-modality isointense infant brain image segmentation," *NeuroImage*, vol. 108, pp. 214–224, Mar. 2015.

[32] X. Wu, H. Wang, W. Tan, D. Wei, and M. Shi, "Dynamic allocation strategy of VM resources with fuzzy transfer learning method," *Peer-to-Peer Netw. Appl.*, vol. 13, no. 6, pp. 2201–2213, Nov. 2020.
[33] A. Kunimatsu, K. Yasaka, H. Akai, H. Sugawara, N. Kunimatsu, and O. Abe, "Texture analysis in brain tumor MR imaging," *Magn. Reson. Med. Sci.*, vol. 21, no. 1, pp. 95–109, 2022.
[34] M. K. Islam, M. S. Ali, M. S. Miah, M. M. Rahman, M. S. Alam, and M. A. Hossain, "Brain tumor detection in MR image using superpixels, principal component analysis and template based K-means clustering algorithm," *Mach. Learn. Appl.*, vol. 5, Sep. 2021, Art. no. 100044.
[35] M. Nickparvar, 2021, "Brain tumor MRI dataset," Kaggle. Accessed: Dec. 10, 2023, doi: 10.34740/KAGGLE/DSV/2645886.
[36] J. Cheng, Apr. 2, 2017, "Brain tumor dataset," Figshare. Accessed: Dec. 17, 2023, doi: 10.6084/m9.figshare.1512427.v5.

RAJA WASEEM ANWAR received the Ph.D. degree from Universiti Teknologi Malaysia (UTM), Malaysia. He is currently an Assistant Professor in cybersecurity with the Department of Computer Science, German University of Technology (GUtech), Muscat, Oman. His research interests include information security, cyber security for cyber-physical systems, trust, security in wireless sensor networks, machine learning, and the IoT. In addition, he received several awards in teaching, research, and academic excellence. He has been invited to serve in many international conferences, journals, and program committees.

MOHAMMAD ABRAR (Senior Member, IEEE) received the Ph.D. degree in computer science from Universiti Teknologi Malaysia, in 2013. He is currently a Distinguished Researcher in the field of computer science, specializing in artificial intelligence, neural networks, classification, and federated learning. With a keen interest in cutting-edge technologies, he has made remarkable contributions to the field of AI. His expertise lies in the development and application of neural networks, specifically in the area of classification. His research work has been published in reputable conferences and high-impact research journals, making a significant impact on the scientific community. His dedication and expertise in federated learning have paved the way for advancements in distributed machine learning algorithms, ensuring privacy-preserving, and efficient training processes across decentralized data sources. His research findings have practical implications for various domains, including healthcare, finance, and telecommunications.

FAIZAN ULLAH received the Ph.D. degree in computer science from the Department of Computer Science and Software Engineering, International Islamic University Islamabad, Pakistan. He is currently a Postdoctoral Researcher with Forschungszentrum Jülich, Germany. Previously, he was an Assistant Professor with the Department of Computer Science, Bacha Khan University Charsadda. His research interests include data mining, machine learning, and deep learning—key areas in modern computer science. His work focuses on advancing artificial intelligence by developing computational techniques to extract meaningful insights from complex data, contributing to the broader field of intelligent systems.